JCI The Journal of Clinical Investigation

T cell receptor grafting allows virological control of hepatitis B virus infection

Karin Wisskirchen, … , Maura Dandri, Ulrike Protzer

J Clin Invest. 2019. https://doi.org/10.1172/JCI120228.

Research Article | Immunology | Virology

Graphical abstract

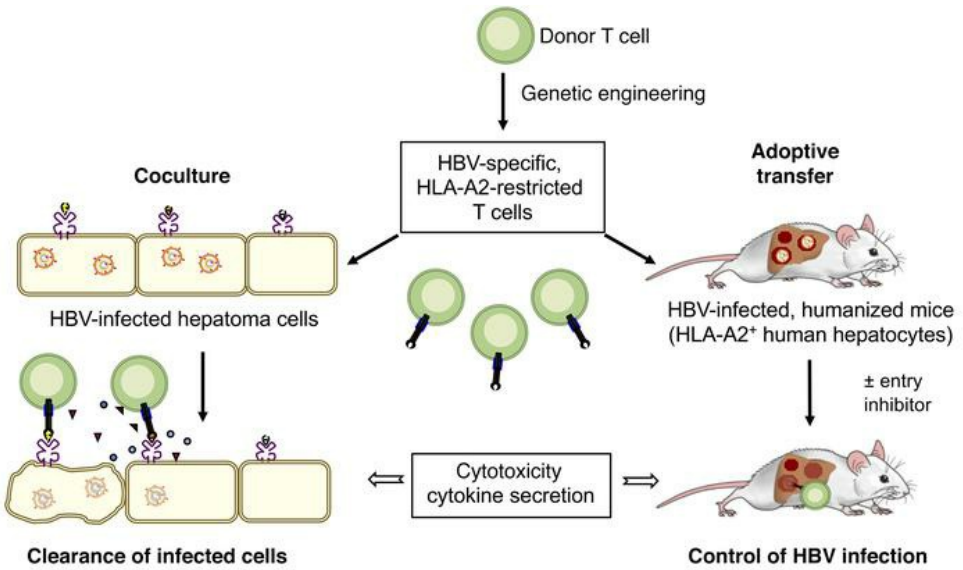

T cell receptor grafting allows virological control of hepatitis B virus infection

Karin Wisskirchen,[1,2,3] Janine Kah,[3,4] Antje Malo,[1] Theresa Asen,[1] Tassilo Volz,[4] Lena Allweiss,[4] Jochen M. Wettengel,[2] Marc Lütgehetmann,[3,5] Stephan Urban,[3,6] Tanja Bauer,[1,2,3] Maura Dandri,[3,4] and Ulrike Protzer[1,2,3]

[1]Institute of Virology, Helmholtz Zentrum München, Munich, Germany. [2]Institute of Virology, School of Medicine, Technical University of Munich, Munich, Germany. [3]German Centre for Infection Research (DZIF), Munich, Hamburg, and Heidelberg partner sites, Germany. [4]1st Department of Medicine, University Medical Center Hamburg-Eppendorf, Hamburg, Germany. [5]Institute of Microbiology, Virology, and Hygiene, University Medical Center Hamburg-Eppendorf, Hamburg, Germany. [6]Department of Infectious Diseases, Molecular Virology, University Hospital Heidelberg, Heidelberg, Germany.

T cell therapy is a promising means to treat chronic hepatitis B virus (HBV) infection and HBV-associated hepatocellular carcinoma. T cells engineered to express an HBV-specific T cell receptor (TCR) may cure an HBV infection upon adoptive transfer. We investigated the therapeutic potential and safety of T cells stably expressing high-affinity HBV envelope– or core–specific TCRs recognizing European and Asian HLA-A2 subtypes. Both $CD8^+$ and $CD4^+$ T cells from healthy donors and patients with chronic hepatitis B became polyfunctional effector cells when grafted with HBV-specific TCRs and eliminated HBV from infected HepG2-NTCP cell cultures. A single transfer of TCR-grafted T cells into HBV-infected, humanized mice controlled HBV infection, and virological markers declined by 4 to 5 log or below the detection limit. Engineered T cells specifically cleared infected hepatocytes without damaging noninfected cells when, as in a typical clinical setting, only a minority of hepatocytes were infected. Cell death was compensated by hepatocyte proliferation, and alanine amino transferase levels peaking between days 5 and 7 normalized again thereafter. Cotreatment with the entry inhibitor myrcludex B ensured long-term control of HBV infection. Thus, T cells stably transduced with highly functional TCRs have the potential to mediate clearance of HBV-infected cells, causing limited liver injury.

Introduction

Worldwide, more than 250 million humans suffer from chronic hepatitis B (CHB), which results in an estimated 880,000 deaths per year caused by secondary complications like liver cirrhosis or hepatocellular carcinoma (HCC) (1). Current therapeutic regimens based on the use of nucleos(t)ide analogs (NUCs) can efficiently suppress viral replication but are unable to eradicate the virus. The so-called covalently closed circular DNA (cccDNA) of hepatitis B virus (HBV) persists as a transcription template in the nucleus of infected cells and reinitiates HBV replication when antiviral treatment is discontinued (2). Hence, therapeutic options are needed, in which cccDNA is eliminated or at least strongly reduced and controlled by the immune system to allow a functional HBV cure and prevent relapse (3).

During acute, resolving hepatitis B, a strong immune response is mounted, with T cells being key to clearance of the virus (4). In CHB, by contrast, the scarce and oligoclonal T cell response against HBV fails to control the virus and prevent disease progression (5). T cells have been shown to kill infected hepatocytes and secrete cytokines that control virus replication in a noncytolytic fashion by silencing (6–8) — but also destabilizing — cccDNA (9, 10). In addition, killing of HBV-infected cells will promote compensatory cell proliferation that in turn favors further cccDNA loss by cell division (11).

Restoring a potent T cell response by adoptive T cell therapy is an interesting therapeutic option (12, 13). The concept of transferring adaptive immunity to control HBV has already been applied successfully in patients with CHB who underwent stem cell transplantation and received bone marrow from HBV-immune donors (14–16). Since allogeneic stem cell transplantation is limited by its severe side effects like graft-versus-host disease and a high rate of mortality, alternative approaches are required. Genetic engineering of autologous T cells to express HBV-specific receptors is an attractive alternative to treat CHB, prevent HBV-related complications, or treat HBV-related HCC (17).

We have already demonstrated that T cells expressing a chimeric antigen receptor binding the antigenic loop within the "S" domain of all HBV envelope proteins selectively eliminated HBV-infected and thus cccDNA-positive target cells (18, 19). It has also been shown that T cells from HBV-infected patients can be engrafted with T cell receptors (TCRs) against the envelope or the core protein and become activated upon recognition of HBV peptides (20, 21). Moreover, a significant reduction of HBV infection in humanized mice was recently demonstrated after repeated adoptive transfers of human T cells engineered to express HBV-specific TCRs via mRNA electroporation (22). How-

Authorship note: KW, JK, MD, and UP contributed equally to this work.
Conflict of interest: UP, KW, and AM hold shares of and serve as advisors for SCG Cell Therapy Pte. Ltd. SU holds patent rights on myrcludex B (Bulevirtide) ("Hydrophobic modified pres-derived peptides of hepatitis B virus [HBV] and their use as HBV and HDV entry inhibitors." US9562076B2).

Submitted: February 5, 2018; **Accepted:** April 25, 2019; **Published:** June 10, 2019.
Reference information: *J Clin Invest*. https://doi.org/10.1172/JCI120228.

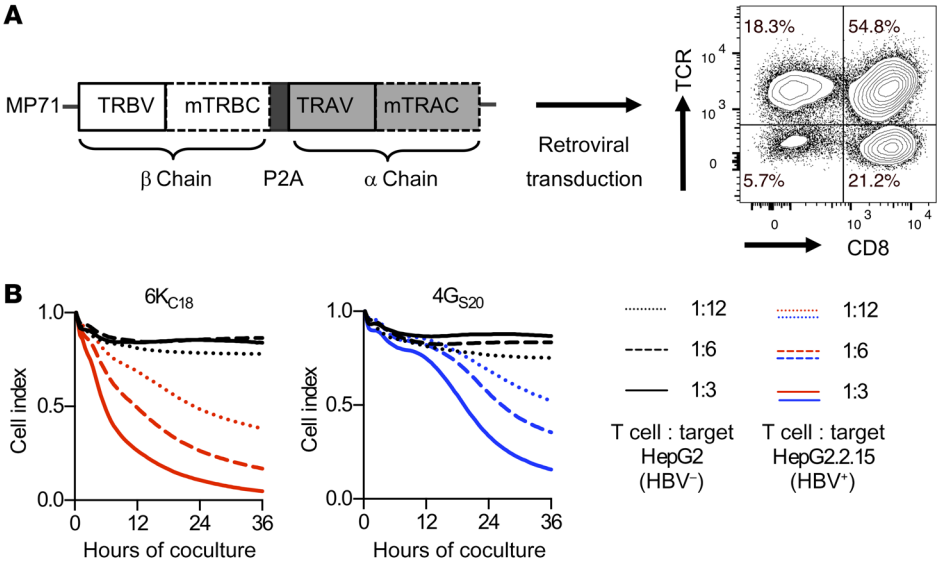

Figure 1. Genetic engineering and analysis of HBV-specific T cells. (**A**) Codon-optimized TCR α (TRAV) and β (TRBV) chains of high-affinity TCRs were cloned into the retroviral vector MP71. Murine constant domains (mTRBC and mTRAC) and insertion of additional cysteines were used to increase pairing. After retroviral transduction, T cells were stained for mTRBC, and TCR expression was quantified by flow cytometry. (**B**) A functional comparison scored 11 TCRs directed against the HBV peptides core$_{18-27}$, S$_{20-28}$, and S$_{172-180}$ (21). The TCRs 6K$_{C18}$ and 4G$_{S20}$ were identified as having the highest functional avidity and were therefore chosen for further analyses: Parental HepG2 or HBV$^+$ HepG2.2.15 target cells were cocultured with increasing numbers of TCR-grafted T cells. Killing of target cells was determined by detachment from the plate using a real-time cell analyzer (XCelligence) and is given as the normalized cell index relative to the starting point of the coculture. HBV-negative target cells cocultured with TCR-grafted T cells are shown as black lines. HBV-positive target cells cocultured with 6K$_{C18}$-transduced T cells are shown in red and 4G$_{S20}$-transduced T cells in blue. Data are presented as mean values of quadruplicate cocultures (n = 4).

ever, because of the transient expression of the TCR and the high numbers of infected cells present in that experimental setting, the antiviral effects remained limited, and HBV rebound was observed within 10 days of the last T cell injection. It is most likely that a more sustained T cell activity, ideally combined with strategies aiming at blocking new infection events (23), is required to achieve a more profound and durable control of HBV infection. We recently reported the cloning, characterization, and permanent expression of a set of 11 HBV-specific TCRs and determined their functional avidity (21). This allowed us to identify the most promising TCRs for adoptive T cell therapy.

In the present study, we aimed to determine the potential of T cells grafted by retroviral vector transduction with HBV-specific TCRs to clear HBV-infected cells without damaging noninfected neighboring cells. Furthermore, we combined T cell therapy with the virus entry inhibitor myrcludex B (MyrB) (24) to restrict the spreading of new virus after T cell control of HBV infection and showed that T cells grafted with selected, high-avidity TCRs were able to control HBV infection in cultured hepatocytes and in vivo in the livers of HBV-infected humanized mice.

Results

Core- and S-specific TCRs confer HBV specificity upon retroviral transduction. HLA-A2–restricted HBV envelope– or core–specific TCRs were cloned as gene-optimized constructs into a retroviral vector. TCR-transgenic T cells were generated by retroviral transduction, resulting in high expression of both TCRs on CD4$^+$ as well as CD8$^+$ T cells (Figure 1A). We compared the functional avidities of 11 TCRs in extensive analyses, resulting in a functionality rating that was as described in detail in Wisskirchen et al. (21) (Supplemental Table 1; supplemental material available online with this article; https://doi.org/10.1172/JCI120228DS1). The core$_{18-27}$ (C$_{18}$)–specific TCR 6K$_{C18}$ and the S$_{20-28}$ (S$_{20}$)–specific TCR 4G$_{S20}$ were selected for comprehensive testing of their antiviral activity. Transduced T cells killed stable HBV-replicating hepatoma cells in cocultures at an effector-to-target (E/T) ratio as low as 1:12. At an E/T ratio of 1:3, core-specific, 6K$_{C18}$-grafted T cells eliminated 50% of HBV-replicating cells after 6 to 7 hours. S-specific, 4G$_{S20}$-grafted T cells showed slower kinetics and required approximately 20 hours (Figure 1B). Thus, endogenously processed peptides were readily recognized by both receptors and activated T cell effector functions.

TCR-grafted T cells efficiently target HBV-infected cells in vitro. Our next step was to assess the antiviral capacity of TCR-grafted T cells on HepG2 cells stably expressing the HBV entry receptor NTCP (HepG2-NTCP) and infected with HBV. On the basis of titration experiments (Supplemental Figure 1, A–F), we incubated the HBV-infected cells with TCR-grafted T cells at an E/T cell ratio of 1:2 and tested whether this would be sufficient to eliminate HBV-infected cells. After 6 and 10 days of coculture, viral HBsAg and HBeAg were no longer detected in cell culture media, respectively (Figure 2, A and B), whereas secreted and intracellular viral relaxed circular DNAs (rcDNAs) were largely reduced (Figure 2, C and D). Most important, the persistence form of the viral DNA — cccDNA — became undetectable by quantitative PCR (qPCR) after 10 days (Figure 2E). A more prominent effect on cccDNA than on rcDNA was expected, since rcDNA is protected from DNase activity within the HBV capsid (18). The amount of extracellular rcDNA even increased temporarily when infected cells were lysed by HBV-specific T cells (Figure 2C), probably because of the release of nonenveloped DNA-containing capsids (25).

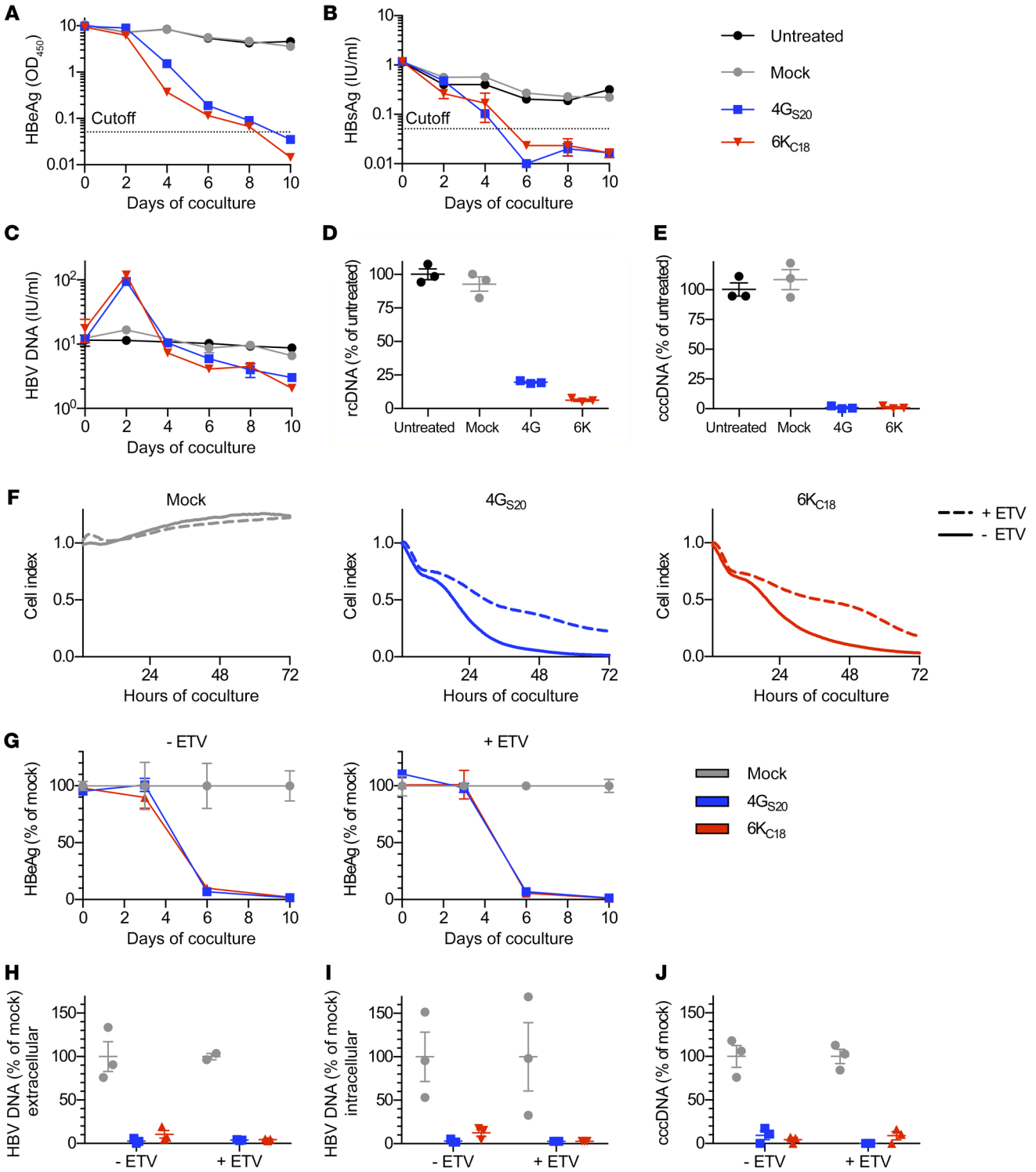

Figure 2. Antiviral effect of TCR-grafted T cells on HBV-infected cells. HepG2-NTCP cells were infected with HBV at a MOI of 100. After 2 weeks, T cells grafted with HBV S–specific TCR $4G_{S20}$ (blue squares) or HBV core–specific TCR $6K_{C18}$ (red triangles) or nontransduced T cells (mock, gray circles) were added for 10 days at an E/T ratio of 1:2. Medium was changed every other day and used to determine (**A**) HBeAg and (**B**) HBsAg by diagnostic ELISA. (**C**) HBV rcDNA contained in virions that had been secreted was extracted from cell culture supernatant every other day, and DNA extracted from cell lysates on day 10 was used to determine (**D**) intracellular HBV rcDNA and (**E**) nuclear cccDNA by qPCR. (**F**–**J**) Cells were infected at a MOI of 500. One week after infection, cells were treated with 0.1 μM ETV twice a week for 3 weeks. (**F**) Killing of target cells was measured using a real-time cell analyzer and is reported as the normalized cell index relative to the starting point of the coculture. E/T of 1:1. (**G**–**J**) Medium was changed every 3 to 4 days, and values were normalized for cocultures treated with mock T cells. (**G**) HBeAg in supernatant of cocultures without or with ETV pretreatment. (**H** and **I**) HBV rcDNA contained in virions secreted into the cell culture medium or extracted from cell lysates on day 10, and (**J**) nuclear cccDNA was determined using qPCR. Data are presented as mean values from triplicate cocultures (n = 3).

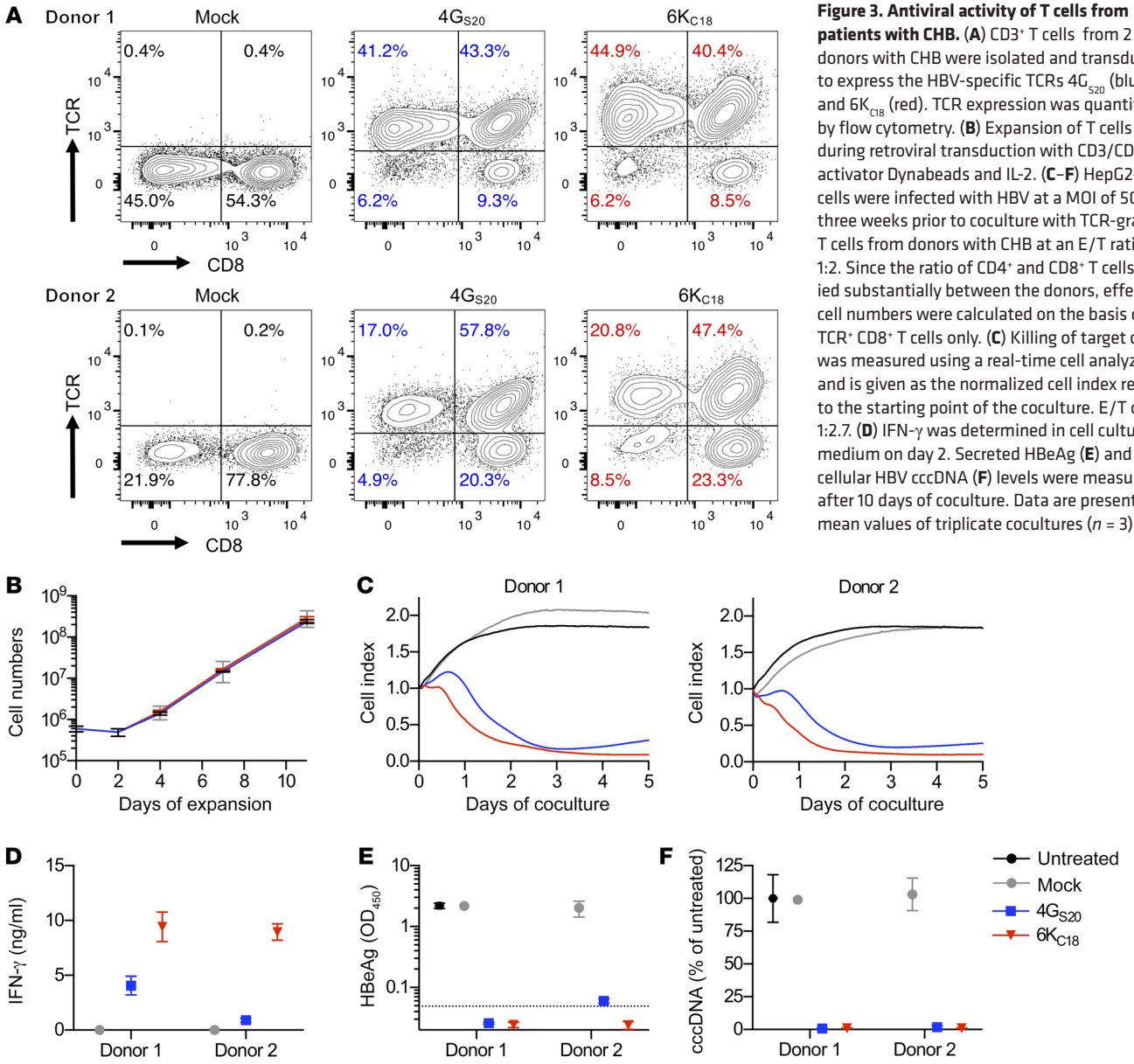

Figure 3. Antiviral activity of T cells from patients with CHB. (**A**) CD3$^+$ T cells from 2 donors with CHB were isolated and transduced to express the HBV-specific TCRs $4G_{S20}$ (blue) and $6K_{C18}$ (red). TCR expression was quantified by flow cytometry. (**B**) Expansion of T cells during retroviral transduction with CD3/CD28 T activator Dynabeads and IL-2. (**C**–**F**) HepG2-NTCP cells were infected with HBV at a MOI of 500 three weeks prior to coculture with TCR-grafted T cells from donors with CHB at an E/T ratio of 1:2. Since the ratio of CD4$^+$ and CD8$^+$ T cells varied substantially between the donors, effector cell numbers were calculated on the basis of TCR$^+$ CD8$^+$ T cells only. (**C**) Killing of target cells was measured using a real-time cell analyzer and is given as the normalized cell index relative to the starting point of the coculture. E/T of 1:2.7. (**D**) IFN-γ was determined in cell culture medium on day 2. Secreted HBeAg (**E**) and intracellular HBV cccDNA (**F**) levels were measured after 10 days of coculture. Data are presented as mean values of triplicate cocultures (n = 3).

To assess whether pretreatment with antivirals would influence antiviral T cell activity, we treated HBV-infected cells with the NUC entecavir (ETV) for 3 weeks before adding TCR-grafted T cells. Although killing of ETV-treated target cells within 72 hours was reduced (Figure 2F), the overall antiviral effect of HBV-specific T cells remained equally pronounced compared with the effect of T cells without NUC treatment (Figure 2, G–J). Thus, both core- and S-specific T cells generated by genetic engineering were capable of eliminating HBV-infected cells, even after treatment with NUCs.

HBV-specific TCRs mediate the redirection of T cells from patients with CHB. Adoptive T cell therapy imposes the challenge of creating an autologous T cell product from a patient who has high levels of circulating viral antigen and chronic inflammatory liver disease. Therefore, we used PBMCs from 2 patients with CHB, grafted T cells with the 2 selected TCRs, and evaluated the antiviral potency of the T cells. We found that the T cells could be transduced as efficiently as T cells from healthy donors (Figure 3A and Figure 1A). T cells expanded by more than 200-fold, starting from fewer than 1 million cells, irrespective of the donor or the TCR being expressed (Figure 3B). $4G_{S20}$- and $6K_{C18}$-grafted T cells killed infected cells (Figure 3C) and secreted up to 10 ng/ml IFN-γ within 2 days (Figure 3D). After 10 days of coculture, secreted HBeAg became negative, with the exception of $4G_{S20}$ T cells obtained from donor 2, in which very low levels were still detected, but cccDNA was no longer detectable (Figure 3, E and F). Importantly, T cells from patients with CHB did not inherently contain a relevant number of functional HBV-specific T cells before TCR grafting, as we observed no antiviral activity of mock-transduced T cells.

Adoptive T cell therapy using T cell receptors requires that the TCR be customized to fit the patient's HLA type. Therefore, we asked whether our high-affinity TCRs would recognize peptide presented on different HLA-A*02 subtypes (Supplemental Figure 2). In total, we found that the TCR $4G_{S20}$ or $6K_{C18}$ recognized their cognate peptide on 9 of 12 or 7 of 12 tested HLA-A*02-subtypes, respectively, including

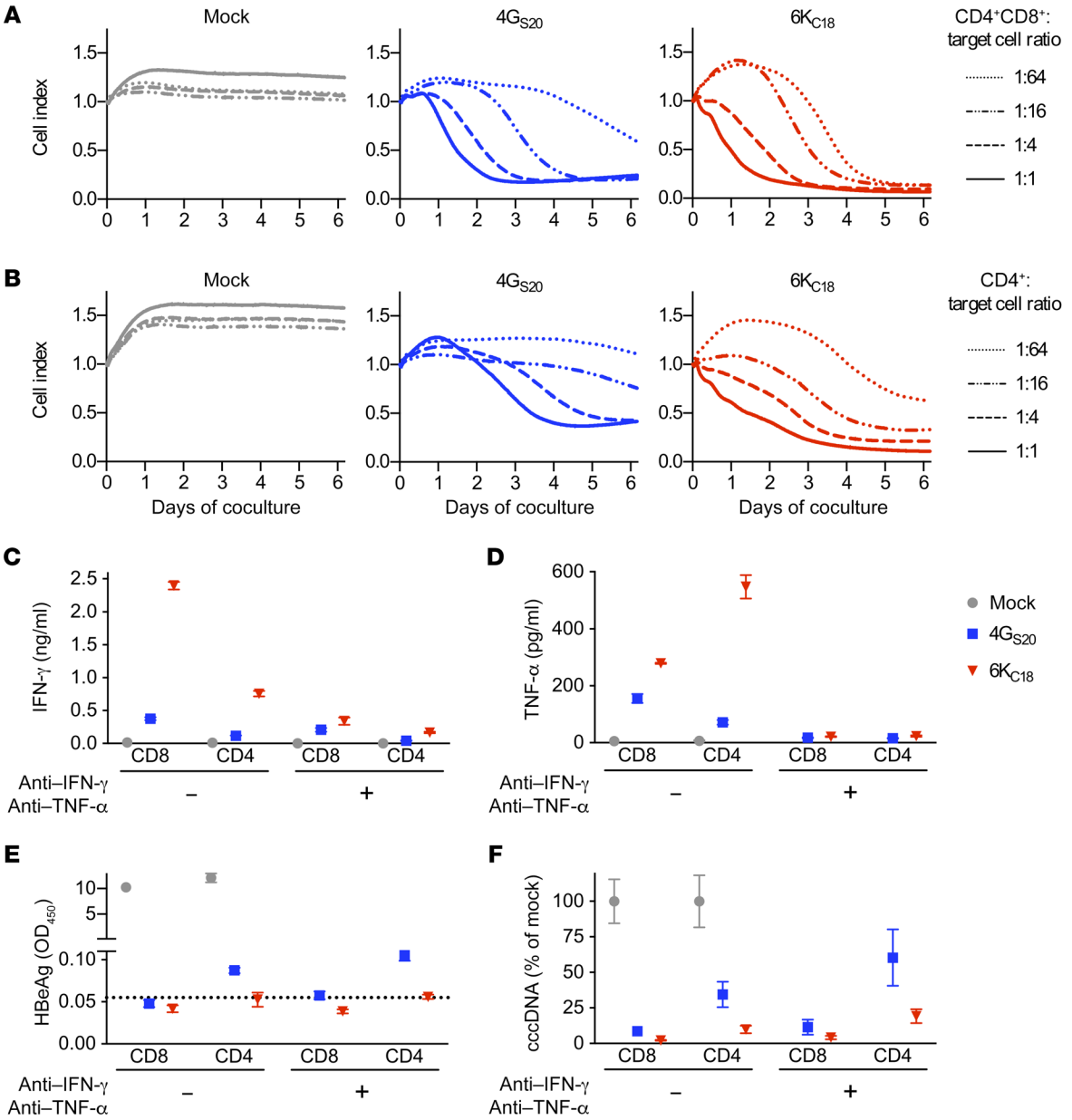

Figure 4. Antiviral activity of different TCR-grafted T cell subsets. HepG2-NTCP cells were infected with HBV at a MOI of 500. After 2 to 3 weeks, T cells grafted with the TCRs 4G$_{S20}$ (blue squares) or 6K$_{C18}$ (red triangles) or nontransduced T cells (mock, gray circles) were added at decreasing E/T ratios. (**A** and **B**) Killing of target cells determined from the bottom of the 96-well plate was measured in real-time (xCELLigence) and is given as the normalized cell index relative to the starting point of the coculture with CD4$^+$CD8$^+$ T cells (**A**) or CD4$^+$ T cells only (**B**). (**C**–**F**) CD8$^+$ and CD4$^+$ T cells were separated by positive magnetic cell sorting and added at an E/T ratio of 1:2. Cytokine-blocking antibodies against IFN-γ (10 ng/ml) or TNF-α (5 ng/ml) were given every other day when medium was exchanged. (**C** and **D**) IFN-γ and TNF-α were measured in the cell culture medium after 2 days. (**E**) Secreted HBeAg and (**F**) intracellular HBV cccDNA levels were measured after 10 days of coculture. Data are presented as mean values (**A** and **B**) or mean values ± SEM (**C**–**F**) of triplicate cocultures (n = 3).

subtypes A*02:03, A*02:06, and A*02:07, which are most frequently found in the Asian population. Taken together, these TCRs conferred HBV specificity to T cells from donors with CHB with a performance comparable to that of T cells from healthy donors and can be applied to patients with different HLA-A*02 subtypes.

TCR-grafted CD4$^+$ and CD8$^+$ T cells show antiviral activity. To quantify the contribution of CD4$^+$ T cells to the control and elimination of HBV, infected cells were first cocultured either with a mixture of CD4$^+$ and CD8$^+$ TCR-grafted T cells or with TCR-grafted CD4$^+$ T cells alone. The combination of CD4$^+$ and CD8$^+$ T cells grafted with either TCR killed infected cells, even at a starting E/T ratio as low as 1:64 (Figure 4A). CD4$^+$ T cells were also able to kill infected cells, although less efficiently, requiring a 4-fold higher number of transduced T cells, i.e., a higher E/T ratio (Figure 4B). Cytotoxic effector function of core-specific T cells started immediately after onset of the coculture, whereas that of S-specific T cells only started 1 or 2 days later. Secreted HBeAg declined 2–3 days after the onset of cytotoxicity (Supplemental Figure 3, A and

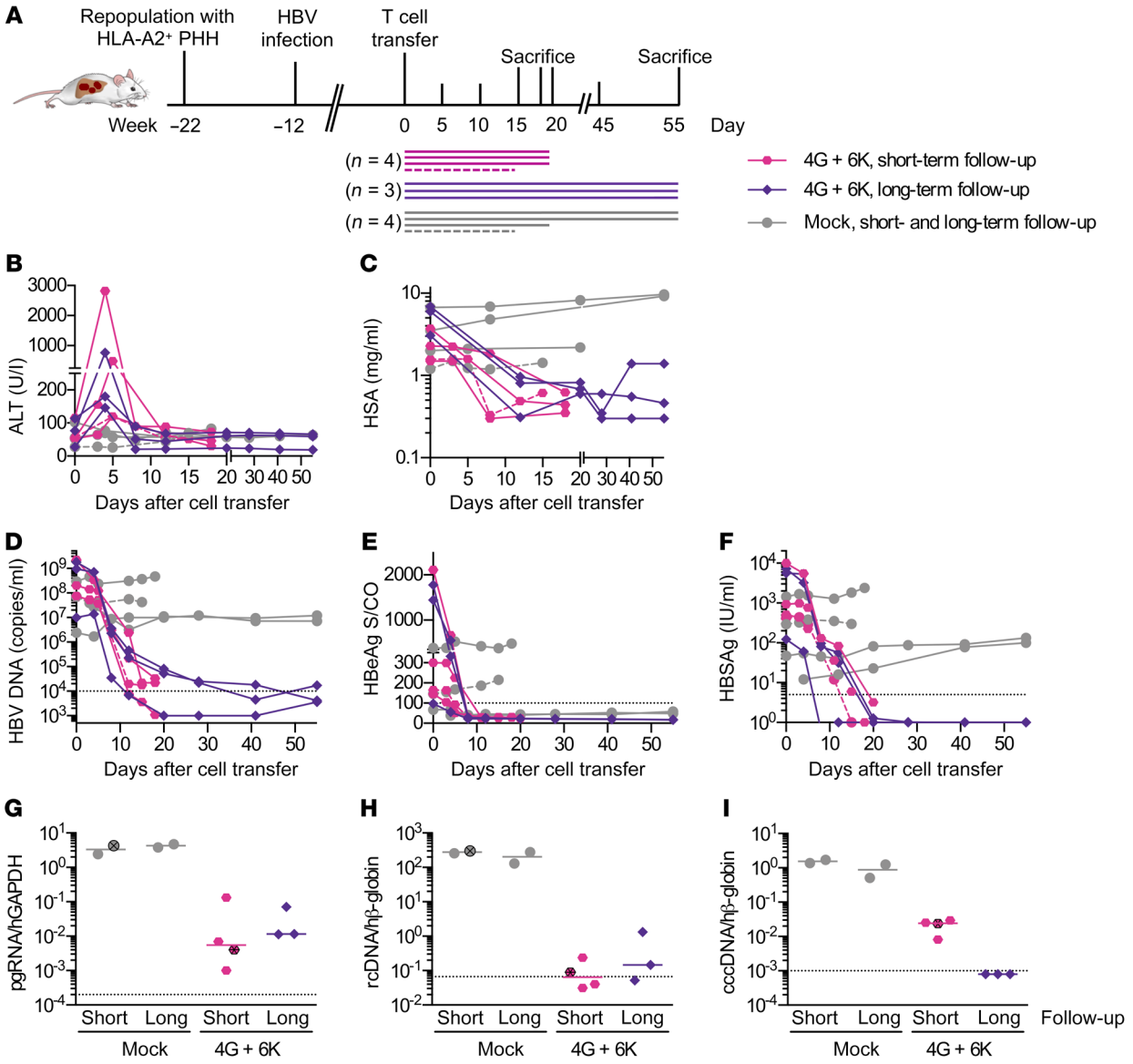

Figure 5. Antiviral activity of TCR-grafted T cells in HBV-infected humanized mice. (**A**) USG mice were repopulated with HLA-A*02–matched PHHs, infected with 1×10^7 HBV virions, followed until a stable viremia was established (weeks 12–14), and injected with 2×10^6 TCR-grafted T cells (1×10^6 with $6K_{C18}$ plus 1×10^6 with $4G_{S20}$; colored symbols; $n = 7$) or with equal numbers of mock-treated human T cells (gray circles; $n = 4$). Four mice were sacrificed within three weeks (short-term follow-up, pink hexagons), and three mice were sacrificed eight weeks (long-term follow-up, purple diamonds) after T cell transfer, respectively. Two of eleven mice received a second dosage of either effector cells or mock cells and were sacrificed on day fifteen (indicated by dashed lines in **A**–**F** and crossed dots in **G**–**I**). (**B**) ALT activity and progression of (**C**) HSA or (**D**) HBV DNA in sera. (**E** and **F**) HBeAg and HBsAg levels were determined by immunoassay. **(G–I)** Intrahepatic HBV RNA and DNA transcripts were quantified by qPCR. (**G**) Levels of HBV pgRNA were normalized to human GAPDH (hGAPDH) RNA. (**H** and **I**) rcDNA and cccDNA were quantified relative to an HBV plasmid standard curve and normalized to human β-globin (hβ-globin). Each data point or longitudinal line represents 1 mouse. Dotted lines represent the technical cutoff of the respective test. For DNA and RNA analyses, dotted lines indicate the lower limit of detection (LLoD), defined as 35 cycles of RT-PCR for pgRNA and 10 HBV rcDNA or cccDNA copies per 1000 or more human β-globin copies.

B). A direct comparison of both T cell types revealed that $CD8^+$ T cells mainly produced IFN-γ and $CD4^+$ T cells TNF-α in particular when using the TCR $4G_{S20}$ (Figure 4, C and D, and Supplemental Figure 3C). Overall, $CD8^+$ T cells showed a stronger antiviral effect, and $CD4^+$ T cells that carried the TCR $6K_{C18}$ were more efficient than $CD4^+$ T cells grafted with the TCR $4G_{S20}$ (Figure 4, E and F, and Supplemental Figure 3, D and E). Taken together, $CD8^+$ as well as $CD4^+$ T cells were able to kill HBV-infected cells when expressing a TCR with a high functional avidity.

TCR-grafted T cells clear HBV-infected cells mainly by direct cytotoxicity. Both cytotoxicity and secretion of cytokines by T cells play a role in viral clearance. To determine the contribution of noncytotoxic, cytokine-mediated antiviral activity of TCR-grafted T cells, we used cytokine-depleting antibodies in our in vitro infection model. The antibodies reduced the amount of IFN-γ by approximately 60% and 90% for $4G_{S20}$- and $6K_{C18}$-expressing T cells, respectively, and almost completely depleted TNF-α from the cell culture medium (Figure 4, C and D, and Supplemental Figure 4, A and B). A reduc-

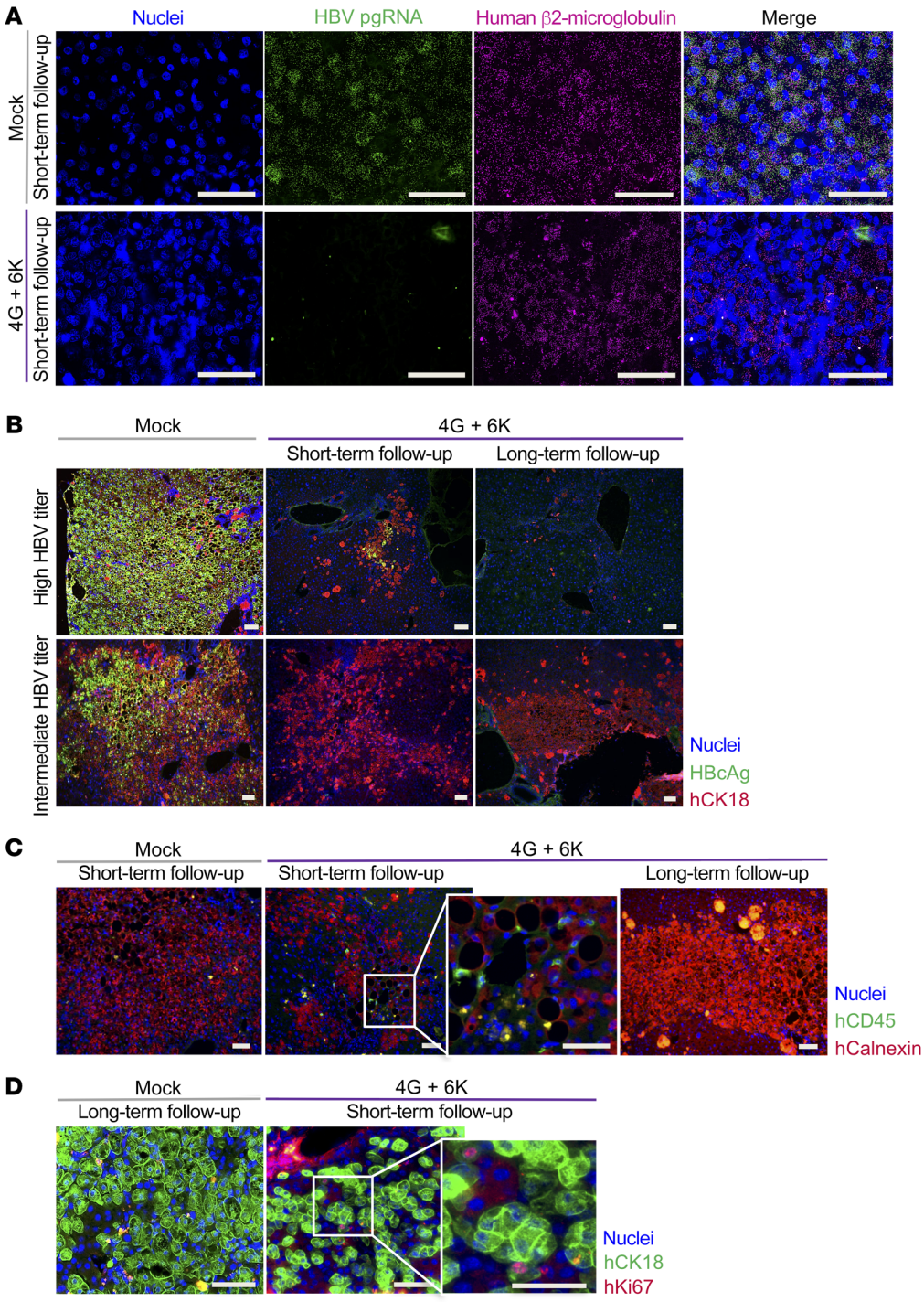

Figure 6. In situ analysis of antiviral effects of TCR-grafted T cells in humanized livers. Liver tissue from HBV-infected mice treated with mock-transduced T cells or 2×10^6 HBV-specific T cells (1×10^6 with $6K_{C18}$ plus 1×10^6 with $4G_{S20}$) were used from days 18–19 (short-term follow-up) or day 55 after T cell transfer (long-term follow-up). (**A**) RNA in situ hybridization for HBV pgRNA (green) and human β2-microglobulin (magenta) against nuclei staining (blue) was performed to determine the occurrence of HBV-specific RNA transcripts. (**B**) As indicated, mice were categorized as having a high (10^9 to 10^{10} copies/ml) or low (10^7 to 10^8 copies/ml) HBV titer. Representative immunohistochemical staining for cell nuclei (blue), HBV core protein (green), and human CK18 (hCK18) (red). (**C**) Human $CD45^+$ cells (green) were stained against human calnexin (hCalnexin) (red) as a marker for human hepatocytes and cell nuclei (blue). (**D**) To determine potential proliferation in mice treated with T cells, staining for cell nuclei (blue), human CK18 (green), and human Ki67 (hKi67) (red) was done. Scale bars: 50 μm.

tion of secreted HBeAg remained similar when cytokines were depleted (Figure 4E and Supplemental Figure 4C). Although cccDNA levels remained strongly reduced when cocultures with $CD8^+$ T cells were treated with cytokine-blocking antibodies, cytokine removal reduced the capacity of $CD4^+$ T cells to eliminate cccDNA (Figure 4F). A detailed comparison of $4G_{S20}$- and $6K_{C18}$-expressing T cells showed that cccDNA clearance was reduced by a factor of 1.5 to 2 when IFN-γ and TNF-α were neutralized (Figure 4F). This indicated that TCR-grafted $CD8^+$ T cells mainly clear HBV by direct cytotoxicity, whereas TCR-grafted $CD4^+$ T cells elicit both a cytotoxic and a prominent noncytotoxic cytokine–mediated effect.

The high cytolytic T cell activity in vitro raised the concern of potential bystander killing of noninfected cells. To address this concern, HBV-infected HepG2-NTCP cells infected at a MOI of 100 to obtain approximately half of the cells productively infected with HBV (26) were mixed with noninfected cells at different ratios. Interestingly, we found that $4G_{S20}$-specific T cells were not activated when only 20% of the cells were derived from the infection cell batch, whereas the $6K_{C18}$ T cells still were activated (Supplemental Figure 5, A–C). For both receptors, $4G_{S20}$ and $6K_{C18}$, killing increased with direct proportionality to the percentage of cells from the infected batch (Supplemental Figure 5, A and B). When T

cells were activated for 24 hours by coculture with HepG2-NTCP cells, which had been infected at a MOI of 500 and transferred to noninfected cell cultures, we observed no bystander killing, although T cells remained active on infected cells (Supplemental Figure 5D). These data provided no indication of nonspecific activity of our TCR-grafted T cells.

Transfer of TCR-grafted T cells results in a strong reduction of HBV markers in vivo. For the clinical success of adoptive T cell therapy for CHB, it is important that transferred T cells migrate to the liver, exert their effector function, and eliminate HBV, while maintaining liver function despite a loss of infected hepatocytes. In a first set of experiments, we used human liver chimeric USG mice harboring HLA-A*02–positive human hepatocytes to assess the antiviral activity of T cells stably expressing the selected HBV-specific TCRs. Mice were infected with HBV for 12 weeks and displayed median viral titers of 1.4×10^8 (2.4×10^6 to 2.2×10^9) HBV DNA copies/ml before the mice received a single injection of either 2×10^6 mock-transduced or 1×10^6 6K and 1×10^6 4G-grafted T cells. These mice were followed for a short period of 15 to 20 days or for a longer period of 55 days (Figure 5A). Two additional mice (1 mouse that had received TCR-grafted T cells before and 1 mock-treated control mouse) received a second injection of T cells on day 5 and were sacrificed on day 15. We observed that alanine aminotransferase (ALT) levels were increased between days 3 and 7 after T cell transfer in all mice that had received HBV-specific T cells, indicating transient liver damage (Figure 5B). Liver damage was accompanied by a less than 10% transient reduction in body weight (Supplemental Figure 6A). Mock-treated animals had ALT levels comparable to those of untreated liver chimeric mice, indicating that no alloreaction was caused by the transferred T cells. In these high viremic, HBV-infected mice treated with TCR-grafted T cells, HSA levels decreased substantially (average of 5.7-fold) (Figure 5C). Nevertheless, HSA levels started to slowly rebound in some animals (Figure 5C). Within the first 3 weeks after T cell transfer, viremia decreased by more than 4 $\log_{10}$ (Figure 5D), and HBeAg and HBsAg dropped below the limit of detection in most animals (Figure 5, E and F). At sacrifice, HBeAg proved nonreactive in 6 of 7 mice and HBsAg in 3 of 7 mice treated with TCR-grafted T cells, and the strong reduction of HBV DNA viremia was confirmed (Supplemental Figure 6, B–D).

In line with the serological results, intrahepatic analyses of mice treated with effector T cells showed significantly lower levels (median: –3 $\log_{10}$) of intracellular HBV RNA transcripts (Figure 5G) and rcDNA (Figure 5H) compared with levels in mock-treated mice. In all treated mice, intrahepatic cccDNA dropped to very low levels (median: –2 $\log_{10}$) 3 weeks after T cell transfer and became undetectable after 8 weeks of treatment (Figure 5I). The second T cell injection did not have any further effect, as a single injection of TCR-grafted T cells was already sufficient to achieve strong and sustained antiviral effects.

HBV pregenomic RNA (pgRNA) was not detectable by RNA in situ hybridization in liver tissues of mice that were sacrificed on day 18 (Figure 6A). The discrepancy between in situ and qPCR detection may be explained by the different sensitivity levels of the respective assays and by the fact that in situ analysis only reflects the viral state within a limited area of a liver section, since DNA and RNA for PCR analysis were extracted from a larger piece of liver tissue. Immunofluorescence costaining for HBV core protein and human cytokeratin 18 (CK18) (Figure 6B) revealed that nearly all human hepatocytes were HBV positive in control mice with high viral titers, whereas animals with 10-fold lower viral titers (e.g., 2×10^8 HBV DNA copies/ml) had fewer positive cells (Figure 6B, mock-treated group). T cell injection provoked a massive elimination of infected hepatocytes over time in mice with high infection rates (Figure 6B, top panel), whereas in mice with intermediate infection rates at baseline, a large proportion of human hepatocytes survived (Figure 6B, bottom panel). We still detected human $CD45^+$ lymphocytes in liver tissue on day 19, but not after 8 weeks (Figure 6C). Nevertheless, human T cells, especially $CD8^+$ T cells, were still present in the spleens of mice 8 weeks after T cell transfer, although the proportion of TCR^+ T cells had decreased compared with what had been injected into the mice (Supplemental Figure 7, A and B). This could be attributed to downregulation of the TCR after T cell activation or contraction of the population of HBV-specific T cells after most of the infection had been cleared. Of note, Ki67 staining showed the potential of human hepatocytes to proliferate and hence their ability to compensate for the immune-mediated cell loss (Figure 6D). Taken together, these experiments demonstrated that a single injection of T cells grafted with TCRs of high avidity can efficiently reduce HBV infection by promoting the clearance of HBV-infected hepatocytes in vivo.

TCR-grafted T cells have the potential for clinical application. To assess the specificity with which effector T cells stably expressing HBV-specific TCRs target infected hepatocytes in vivo without provoking damage of noninfected neighboring hepatocytes, we used mice in which only a minority of the human hepatocytes was infected. This mimics the clinical situation more closely, in which typically only a low percentage of cells are infected and express HBV core and envelope proteins (27). To obtain partially HBV-infected humanized livers, we stopped the spreading of HBV 5 weeks after virus inoculation by applying the HBV entry inhibitor MyrB. One week later, five mice received TCR-grafted T cells, whereas three animals served as controls and were sacrificed either two weeks ($n = 2$) or thirteen weeks after injection of mock T cells (Figure 7A). To assess whether HBV may relapse after T cell therapy, we stopped MyrB application in 2 mice 3 weeks after T cell transfer and monitored viremia levels for an additional 10 weeks (i.e., until week 19 after infection).

In line with our previous experiments, we found that a single injection of HBV-specific T cells caused transient ALT elevation (Figure 7B) and a concomitant reduction of HSA levels (Figure 7C) in all treated mice, while their body weight remained stable (data not shown). Compared with high-titer HBV-infected mice (Figure 5C), the HSA drop was less pronounced in the partially infected animals, and HSA rebounded to baseline levels within 2 to 3 weeks (Figure 7C), indicating that the hepatocyte loss was limited and promptly compensated by human hepatocyte proliferation. HBV viremia, as well as circulating HBeAg and HBsAg, dropped to borderline detection levels in all animals within 2 weeks after T cell transfer (Figure 7, D–F). When mice received MyrB throughout the experiment, intrahepatic levels of HBV transcripts and DNA were approximately 4-log lower 3 and 13 weeks after transfer of TCR-grafted T cells compared with treatment with mock T cells

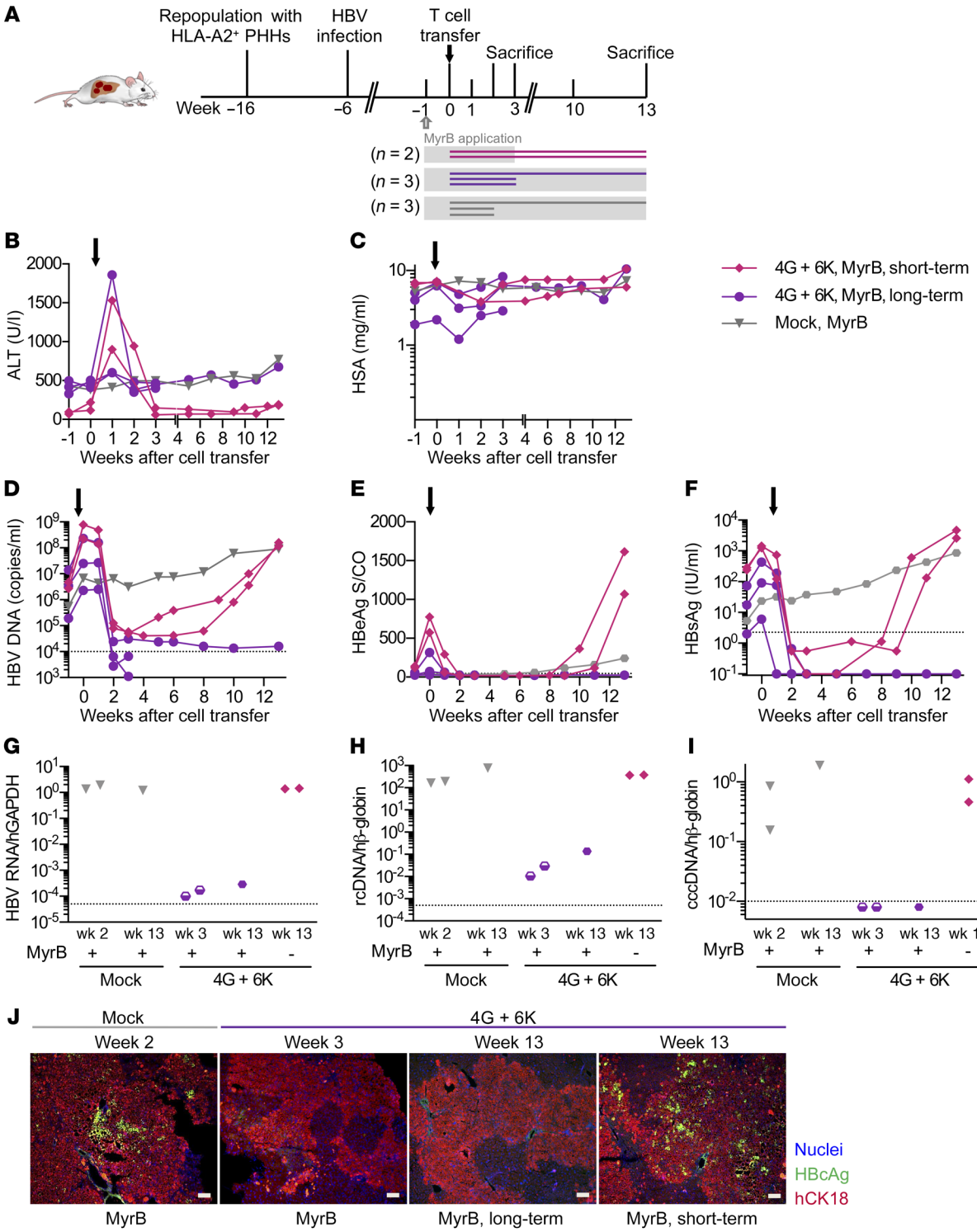

Figure 7. Long-term follow-up of mice partially infected with HBV and treated with HBV-specific T cells and an entry inhibitor. (**A**) USG mice were repopulated with HLA-A*02–matched PHHs and infected with 1×10^7 HBV virions. Viral spreading was stopped at week 5 after infection by administration of MyrB (see Methods) (gray blocks). After 1 week of MyrB application, 2×10^6 TCR-grafted T cells (1×10^6 with $6K_{C18}$ plus 1×10^6 with $4G_{S20}$, $n = 5$) or mock T cells (gray triangles, $n = 3$) were transferred. To address the question of whether mice could be reinfected after treatment with effector T cells, MyrB application was stopped in 2 of 5 mice after 3 weeks (MyrB short-term, pink diamonds, $n = 2$) and followed up until week 13. MyrB was administered continuously in 3 of 5 mice (MyrB long-term, purple circles, $n = 3$). Mice were sacrificed at week 2 or 3 during short-term follow-up or at week 13 during long-term follow-up. Time course of ALT activity (**B**), HSA (**C**), HBV viremia (**D**), HBeAg (**E**), and HBsAg (**F**) in sera followed until week 3 or 13. (**G**) pgRNA levels were normalized to human GAPDH RNA. (**H** and **I**) rcDNA and cccDNA levels were quantified relative to an HBV plasmid standard curve and normalized to human β-globin. Each data point or longitudinal line represents 1 mouse. Dotted lines represent the technical cutoff of the respective test. For DNA and RNA analyses, dotted lines indicate the LLoD, defined as 35 cycles of RT-PCR for pgRNA and 10 HBV DNA or cccDNA copies per 1000 or more human β-globin copies. Dots below the LLoD symbolize undetectable measurements. (**J**) Representative staining of liver tissue slides from mice treated with either mock or 4G plus 6K effector T cells. Scale bars: 50 μm.

(Figure 7, G and I). When MyrB treatment was stopped 3 weeks after T cell injection, all serological HBV markers started to rebound 9 weeks after injection of TCR-grafted T cells (Figure 7, D–F) and reached baseline levels again at 13 weeks (Figure 7, G–I). Costaining for HBcAg and human CK18 revealed that only a minority of human hepatocytes was HBV positive in mice that received MyrB 5 weeks after infection and sacrificed 2 weeks after mock T cell treatment (Figure 7J, left panel). We detected no HBV-positive cells 3 or 13 weeks after transfer of HBV-specific T cells under continuous MyrB treatment, whereas HBV-positive hepatocytes were detected in animals whose MyrB treatment was discontinued (Figure 7I, right panel). These results show that TCR-grafted T cells were able to target HBV-infected cells with high efficiency also when only a minority of human hepatocytes was infected. The lack of off-target effects also indicated high specificity of TCR-redirected T cells. Most important, HBV infection was fully controlled after adoptive transfer of HBV-specific T cells when MyrB was continuously administered.

Discussion

T cell therapy for CHB aims to supplement a patient's lacking or functionally exhausted HBV-specific T cell repertoire to achieve HBV control. In this study, we demonstrate that T cells genetically engineered to stably express HBV-specific TCRs with high functional avidity (21) are able to eliminate HBV-infected cells with high efficiency and specificity. Although our TCRs were cloned from European donors, testing them on different HLA-A2 subtypes showed a broad applicability irrespective of the patient's ethnicity. HBV-specific T cells obtained using T cells from healthy volunteers or from patients with CHB and expanded to clinically relevant numbers were equally efficient and able to eliminate HBV-infected cells. Importantly, a single adoptive T cell transfer combined with administration of the HBV entry inhibitor MyrB was able to achieve long-term control of HBV infection in HBV-infected humanized mice.

Currently approved polymerase inhibitors are well tolerated and effectively suppress HBV replication. However, they do not directly affect the HBV persistence form, i.e., the cccDNA demanding additional means to cure hepatitis B (28). T cells grafted with HBV-specific receptors become activated by HBV-expressing hepatoma cell lines (20, 29) or HBV-infected hepatocytes (30) and target HBV persistence (18).

Our TCRs proved to be functional not only on $CD8^+$ but also on $CD4^+$,T cells, and grafting onto healthy volunteers' or CHB patients' T cells led to the elimination of viral antigens as well as cccDNA when cocultured with HBV-infected cells. Both cell types showed cytotoxic and noncytotoxic effector functions, whereas $CD8^+$ T cells mainly produced IFN-γ, and $CD4^+$ T cells produced TNF-α. Thus, the manufacturing of a T cell product for clinical application can be simplified, as purification of $CD8^+$ T cells will not be essential to generate sufficient numbers of antiviral T cells. As it has been shown that inclusion of $CD4^+$ T cells grafted with a chimeric antigen receptor has a synergistic antitumor effect (31), $CD4^+$ T cells engrafted with our MHC-I–restricted high-affinity TCRs that are fully functional without CD8 coreceptor binding (21) will also very likely contribute to the success of adoptive T cell therapy either by direct antiviral activity or by helper function.

Several cytokines, secreted by adoptively transferred T cells or after bystander activation of other immune cells, have been reported to influence HBV gene expression and replication in a noncytolytic fashion (32) by a number of different means (summarized in ref. 33). Albeit, in our experiments, killing of infected cells was the dominant antiviral mechanism eliminating HBV in cell culture and in vivo. However, since IFN-γ could only partially be blocked by antibodies, the noncytolytic effect of TCR-grafted T cells that was recently reported (29, 34) may have been underestimated in our experiments.

In our first in vivo experimental setting, most human hepatocytes (>90%) were infected with HBV, and mice were highly viremic after the virus had had 12 weeks to spread in the immunodeficient animals. In these animals, a large proportion of the human cells was eliminated upon T cell transfer, cccDNA was reduced by more than 95%, and neither HBV core protein nor viral RNAs could be detected anymore in situ in surviving human hepatocytes. Nevertheless, noncytolytic activity of T cells (29, 35) may have contributed to clearing of the HBV infection, since some human hepatocytes may well have lost cccDNA by cell division (11), as demonstrated by positive Ki67 staining, and T cell–derived cytokines may have contributed to purging (10, 29) or silencing (6) of cccDNA molecules.

A concern about HBV-specific T cell therapy is the loss of a significant part of functional liver cells, particularly in patients with liver cirrhosis or end-stage liver disease. After adoptive T cell therapy, adverse events have been observed when the TCR was specific for a tumor-associated (self-) antigen and bound "off-target" to related peptides (36), or when it recognized the cognate antigen "off-organ" on healthy tissue (37). Both scenarios seem unlikely to happen during T cell therapy for CHB, as the viral antigens we were targeting are very distinct from "self-antigens" and are only expressed in hepatocytes. This is supported by the notion that no severe side effects have been observed after the transfer of HBV-specific immune cells into CHB patients with hematological malignancies and normal liver function, in whom bone marrow transplantation led to viral clearance while only causing moderate liver toxicity (14–16). In this regard, we found that despite the capacity of our engineered T cells to clear infected cells, cytotoxicity of the stably transduced T cells was limited, since ALT indicating hepatocyte death increased only transiently in the first week after T cell transfer. Serum HSA reflecting hepatocyte function dropped in correlation with the amount of intrahepatic infection detected. Humanized mice in which (as in a typical clinical setting) the liver was only partially infected neither lost weight nor showed any other signs of distress. Of note, TCR-grafted T cells did not cause any measurable damage of neighboring noninfected cells, since large hepatocyte areas were maintained and HSA rebounded to baseline levels, emphasizing the capacity of human hepatocytes to proliferate and compensate for the immune-mediated cell loss.

The situation was different when virtually all human hepatocytes were infected. Here, we found a significant drop in HSA, indicating a significant reduction in liver function. A fully infected liver, however, is not expected to reflect the situation of the majority of patients with CHB (27). Another limitation of the humanized mouse model is the mismatch of human cytokines and murine receptors that may underestimate the effect of a cytokine storm.

Huang et al. (38) showed in a study including more than 100 HBeAg-negative patients that in those with a viral load below 1×10^6 copies/ml, the amount of HBcAg-positive hepatocytes was less than 20%. Hence, patients who would be considered candidates for the clinical application of T cell therapy should be carefully selected on the basis of their viremia and antigenemia. Nevertheless, a liver biopsy should be obtained to assess the number of HBV-infected cells as well as the extent of preexisting liver inflammation and fibrosis.

Treatment with NUCs only blocks the viral polymerase and production of new viral progeny, but not the transcription of HBV RNA or antigen production per se. Thus, the presentation of HBV antigen is not expected to change substantially, and HBV-specific T cells should remain able to clear infected cells. Our in vitro study proved that the recognition and clearance capacity of TCR-grafted T cells was maintained upon treatment with ETV. Pretreatment with NUCs would even be preferred, since long-term NUC treatment is associated with a lower extent of intrahepatic HBV infection (27). As in our experiments with partially infected mice, we would expect a less pronounced hepatocyte loss in patients who have received NUCs for several years and that this would not impair liver function in noncirrhotic or child A patients. Moreover, treatment with polymerase inhibitors will also reduce inflammation and thereby increase the safety of adoptive T cell therapy. Safety could be further increased if a safeguard molecule was cotransduced and coexpressed with the TCR to allow for rapid depletion of transferred T cells. To limit the circulation of HBV-specific T cells, the application of T cells that only transiently express the HBV-specific TCR after RNA electroporation was explored (22). However, in the same humanized mouse model, TCR-electroporated T cells led to a comparable increase in ALT but, despite several T cell reinjections, did not achieve the same strong antiviral effect as their retrovirally transduced counterparts did (22), an effect that was even lower when resting, noncytolytic T cells were used (34).

The efficacy of our retrovirally transduced T cells carrying high-avidity TCRs was striking in vivo, especially when compared with previous studies (22, 34). These results point out how a different technology used to engineer effector T cells (i.e., careful selection of TCRs [ref. 21] and stable versus transient TCR expression) helps to achieve a higher efficacy of T cell therapy. We needed only a single T cell injection to achieve a sustained drop of HBsAg and HBV DNA (>4 log) in the serum of mice, whereas multiple injections of transiently transduced T cells were needed to achieve a reduction of HBV viremia by a median 1 log, and HBsAg levels barely changed (22).

However, in the absence of adaptive immune responses, even the smallest persisting HBV reservoir eventually led to viral rebound in our mice. To avoid HBV rebound, we combined T cell therapy with administration of the entry inhibitor MyrB and by this means succeeded in maintaining control of HBV infection for the entire 3-month period after T cell transfer. Although in patients with CHB — in contrast to our immune-incompetent mouse model — long-term survival of transferred T cells is more likely and may even be supported by reconstitution of the patient's own anti-HBV immune response, inhibition of new infection events will have a supportive role in the clinical setting as well.

Adoptive T cell therapy of HBV-related diseases is already proceeding toward use in the clinic. Bertoletti and colleagues recently reported T cell therapy for an HLA-A2–positive patient who had received an HLA-A2–negative liver transplant because of HCC and developed metastases from his original HBV S–positive, HLA-A2–positive HCC. This patient was treated with retrovirally TCR-grafted, S_{20}-specific T cells. The therapy was safe, and circulating HBsAg levels decreased (17). Although these study results were very encouraging, the numbers of TCR-grafted, transferred HBV-specific T cells were low (<2.5% within 3.9×10^8 infused cells). With improved retroviral transduction, we can now generate high numbers of HBV-specific T cells stably expressing TCRs (>75% within 2.5×10^8 cells) from fewer than 1 million cells from healthy donors but, as shown here, also from patients with CHB, who would thus be spared the need to undergo leukapheresis.

Taken together, we show that high-affinity HBV-specific T cells could be generated by TCR grafting, irrespective of whether the donor was HBV positive or HBV negative prior to T cell therapy. TCR-grafted T cells have a strong antiviral capacity in cell culture and in vivo, most strongly reducing cccDNA, which is considered a hallmark of virological cure (3). Thus, adoptive T cell therapy that mimics T cell responses in self-limiting HBV infection may result in a functional cure of HBV infection in patients with CHB.

Methods

Retroviral transduction of T cells. Stable 293GP-R30 (RD114 pseudotype) producer cells were generated by transduction with cell culture supernatant from 293GP-GLV9 cells (both provided by BioVec Pharma) (39) that had been transfected with TCR plasmids as described earlier (21). T cells were enriched using human T activator CD3/CD28 Dynabeads (Thermo Fisher Scientific) and prestimulated for 2 days in T cell medium (TCM) containing RPMI, 10% FCS, 1% penicillin-streptomycin, 1% glutamine, 1% sodium pyruvate, 1% nonessential amino acids, and 0.01 M HEPES (all from Thermo Fisher Scientific), supplemented with 300 U/ml IL-2. 0.45-μm-filtered retrovirus cell culture supernatant from stable producer cell lines. The virus supernatant centrifuged at 2000 *g*, 32°C, for 2 hours on culture plates coated with 20 μg/ml RetroNectin (Takara). Retrovirus cell culture supernatant was removed, and T cells were spinoculated onto the retrovirus-coated plate at 1000 *g* for 10 minutes. A second transduction was performed after 24 hours. TCR expression was determined by flow cytometry. Staining was done for 30 minutes on ice in the dark, using the primary antibodies anti–human CD4-APC (clone OKT4, no. 17-0048-42, eBioscience), anti–human CD8-PB (clone DK25, no. PB984, Dako), and anti–mouse TCRβ-PE (clone H57-597, no. 553172, BD Biosciences) diluted in FACS buffer (0.1% BSA in PBS). Cells were analyzed using a FACSCanto II flow cytometer (BD Biosciences), and the data were analyzed with FlowJo 9.2 software.

Coculture with HBV-infected cells. HepG2 cells expressing the sodium-taurocholate cotransporting polypeptide (HepG2-NTCP K7, generated by our group [ref. 26]) were seeded in DMEM (10% FCS, 1% penicillin-streptomycin, 1% glutamine, 1% NEAA) on collagen-coated plates. At 90% confluency, 2.5% DMSO was added to the medium. Cells were infected 2–6 days later with HBV genotype D, subtype ayw purified via heparin column affinity chromatography followed by sucrose gradient ultracentrifugation from HepAD38 cell culture supernatant in the presence of 4.8% PEG overnight at the indicat-

ed number of virions per cell (MOI) and maintained with 1% FCS as a monolayer. For T cell cocultures, medium was changed to DMEM 10% FCS/2% DMSO. T cells were added in equal amounts of TCM (final concentration of 1% DMSO in coculture) at the indicated ratio (E/T) of $6K_{C18}$ (specific for C18-27: FLPSDFFPSV) or $4G_{S20}$ (specific for S20-28: FLLTRILTI) T cells to target cells. For Figure 2, F–J, HepG2-NTCP cells were infected at a MOI of 500. One week after infection, cells were treated with 0.1 μM ETV twice a week for a duration of 3 weeks. For Figure 4, C–F, $CD8^+$ and $CD4^+$ T cells were separated using MACS beads for positive selection of the respective cell type (Miltenyi Biotec) and added at a E/T ratio of 1:2. Cytokine-blocking antibodies against IFN-γ (10 ng/ml, clone B27, no. 506513, BioLegend) or TNF-α (5 ng/ml, clone D1B4, no. 7321, Cell Signaling Technology) were given every other day when medium was exchanged.

Analyses of cocultures. Cytokines in the cell culture supernatant were detected using ELISA kits for IFN-γ and IL-2 (BioLegend) or for TNF-α (BD Biosciences). HBeAg in the cell culture supernatant was measured using the Enzygnost HBe monoclonal assay (Siemens Healthcare Diagnostics). Total DNA was extracted from cells using the NucleoSpin Tissue Kit (Macherey-Nagel) or from cell culture supernatant using a Tecan extraction robot (40). Viral DNA forms were amplified and detected by PCR as described previously (10) and quantified relative to a standard obtained from accredited assays in our diagnostics department. DNA (7.5 μl) was digested with 5 units of T5 exonuclease (New England BioLabs) for 30 minutes at 37°C to eliminate rcDNA before cccDNA quantification.

Real-time cytotoxicity measurement. HepG2 cells (5×10^4) (American Type Culture Collection [ATCC]) or HepG2.2.15 cells (5×10^4) (a gift of Heinz Schaller, University of Heidelberg, Heidelberg, Germany) were prepared as described previously (21), or 4×10^4 infected or noninfected HepG2-NTCP cells were seeded onto 96-well electronic microtiter plates. T cells were added 1–2 days later when target cells had reached confluence. The impedance, which reflects adherence of the target cells to the bottom of the plate, was measured every 15 to 30 minutes using an xCELLigence SP Real-Time Cell Analyzer (ACEA Biosciences).

Adoptive T cell transfer in humanized mice. Human liver chimeric mice were generated using 3-week-old male or female uPA SCID beige IL-2R$\gamma^{-/-}$ (USG) mice (41). They originated from IL-2Rγ–KO mice (The Jackson Laboratory mice, stock no. 003169; C.129S4-Il2rg<tml-Wjl>/J) were backcrossed 10 times with uPA/SCID. These originated from crossing uPA mice [The Jackson Laboratory, stock no. JR2214 (no longer available); B6SJL-TgN(Alb1Plau)144Bri] for 10 generations with SCID beige mice (Taconic model: CBSCBG; C.B-Igh-1b/GbmsTac-Prkdcscid-Lystbg N7). After transplantation of 1×10^6 thawed human HLA-$A2^+$ hepatocytes, the repopulation levels were determined by measuring HSA in mouse serum using the Human Albumin ELISA Quantitation Kit (Bethyl Laboratories). To establish HBV infection, animals received a single intraperitoneal injection of HBV-infectious serum (1×10^7 HBV-DNA copies/mouse; genotype D) 10 weeks after transplantation. For adoptive T cell transfer, T cells were thawed and cultured overnight in AIM-V medium (Gibco, Thermo Fisher Scientific), 2% human AB^+ serum, and 180 IU/ml IL-2. TCR-grafted T cells (2×10^6: 1×10^6 with $6K_{C18}$ plus 1×10^6 with $4G_{S20}$) or equal numbers of mock-treated T cells were injected intraperitoneally into HBV-infected mice. In the first experiment, mice were monitored until days 15–19 (short-term) or day 55 (long-term) after transfer. In the short-term follow-up groups, 1 mouse from each group (both HBeAg 1.5 [S/CO] on day 3 after transfer) received a second injection of 1×10^6 TCR-grafted or mock T cells on day 6 (mice are specified in Figure 5), and 1 mouse received MyrB 5 days before sacrifice. In the second experiment, all mice received MyrB (100 μl; 2 mg/kg) subcutaneously (11, 24) 5 weeks after infection to block the viral spreading and mimic a partial infection in these mice. Within the first 5 days, mice received MyrB daily. After 5 days, mice were treated every other day to avoid reinfection or new infection of noninfected hepatocytes. Blood was taken for analyses of viral antigens, ALT, and viremia as indicated in the Results.

Virological measurements. DNA and RNA were extracted from liver specimens using the Master Pure DNA Purification Kit (Epicentre) and the RNeasy RNA Purification Kit (QIAGEN), respectively. Intrahepatic total viral loads were quantified with the help of primers and probes specific for total HBV DNA, pgRNA, and cccDNA, and the human housekeeping gene *GAPDH* was used for normalization (42). Quantification of HBsAg and HBeAg was performed using the Abbott Architect platform (Abbott, Ireland, Diagnostic Division) at the indicated serum dilutions. HBeAg results are displayed as the signal cutoff (S/CO).

Analysis of biochemical parameters. ALT was measured using the Roche Cobas c111 System. For the measurements, 5 μl serum from the mice was used.

Preparation and staining of splenocytes. Spleens were dissected in cold mTCM (RPMI, 10% FCS supplemented with glutamin, 1% penicillin-streptomycin, 0.1% β-mercaptoethanol, and 1% sodium pyruvate), passed through a 100-μm strainer, and homogenized through a 20-gauge needle. Splenocytes were centrifuged at 300 *g* for 5 minutes at 4°C and incubated in red blood cell lysis buffer for 2 minutes at 37°C to lyse erythrocytes. Reaction was stopped with mTCM. Cells were counted after repeat centrifugation and subsequently stained for anti–human CD8-PE-Cy7 (clone RPA-T8, no. 557746, BD Biosciences), anti–human CD4 Pacific Blue (clone RPA-T4, no. 558116, BD Biosciences), and anti–mouse TRBC-PE (clone H57-597, no. 553172, BD Biosciences). Flow cytometry data were acquired on the BD FACS LSRII System.

Immunofluorescence and RNA in situ hybridization. Human hepatocytes were identified in frozen mouse liver sections using a monoclonal anti–human CK18 mouse antibody (clone DC-10, 11-107-C100, Exbio) or a monoclonal anti–human calnexin rabbit antibody (clone C5C9, no. 2679, Cell Signaling Technology). HBcAg staining was detected with anti–rabbit anti-HBcAg antibodies (polyclonal, no. B0586, Dako Diagnostika), and specific signals were visualized with Alexa 488– or Alexa 555–labeled secondary antibodies (polyclonal, nos. A21429, A11029, and A11034, Invitrogen, Thermo Fisher Scientific) or using the TSA Fluorescein System (PerkinElmer). Nuclear staining was done using Hoechst 33258 (Invitrogen, Thermo Fisher Scientific). Human CD45 staining was performed using a monoclonal anti–mouse CD45 antibody (clone 2B11 plus PD7/26, no. IS751, Dako). Proliferation of human hepatocytes and immune cells was determined using antibodies against human Ki67 (polyclonal, no. ABIN152984, antibodies-online.com, Germany). RNA in situ hybridization was performed on paraformaldehyde-fixed, cryopreserved liver sections using the RNAScope Fluorescent Multiplex Kit (Advanced Cell Diagnostics), with target probes recognizing the pregenomic HBV (assay 442741-C2) and human β2-microglobulin RNA (assay 478171-C3). Stained sections were analyzed with a fluorescence microscope (Biorevo BZ-9000, Keyence) using the same settings for all groups.

Study approval. The use of PBMCs from healthy volunteers was approved by the local ethics board of the University Hospital rechts der Isar (Munich, Germany, G 548/15S), and written informed consent was obtained from all blood donors. Primary human hepatocytes (PHHs) were isolated from rejected liver explants using protocols approved by the ethics committee of the city and state of Hamburg (OB-042/06) in accordance with Declaration of Helsinki principles. Animals were housed under specific pathogen–free conditions according to institutional guidelines under authorized protocols. All animal experiments were approved by the City of Hamburg (G118/16) and conducted in accordance with the European Communities Council Directive (86/EEC) and Animal Research: Reporting of In Vivo Experiments (ARRIVE) standards.

Author contributions

KW and UP designed in vitro experiments. KW, AM, and TA performed in vitro experiments, and KW analyzed data. KW, JK, MD, and UP wrote the manuscript. TB provided and analyzed patients' material. AM established the transduction protocols. JMW produced and purified HBV stocks. JK, MD, KW, and UP designed in vivo experiments. JK conducted in vivo experiments and acquired data. JK and KW analyzed the data. LA and TV generated human chimeric liver mice. ML and LA established RNA in situ hybridization assays. LA and JK performed RNA in situ hybridization assays. SU conceptually contributed to the entry inhibition experiments and provided MyrB for the in vivo experiments. All authors discussed the data and revised the manuscript.

Acknowledgments

This work was supported by the German Research Foundation (DFG) via TRR36 and TRR179 (to UP) and SFB841 and a Heisenberg Professorship (DA1063/3-2, to MD). UP, MD, and SU received funding from the German Center for Infection Research (DZIF) (TTU Hepatitis 05.806, 05.704, 05.815). KW received a maternity leave stipend and a young investigator grant from the DZIF (TTU Hepatitis 05.812). We thank Ke Zhang for generating and Daniela Stadler (both from Helmholtz Zentrum München) for cloning HepG2NTCP cells; Wolfgang Uckert (Technical University of Munich) for providing optimized MP71 constructs; and Michael Ostertag (Technical University of Munich) for creating retrovirus producer cell lines.

Address correspondence to: Ulrike Protzer or Karin Wisskirchen, Institute of Virology, Trogerstrasse 30, 81675 Munich, Germany. Phone: 49.89.4140.6886; Email: protzer@tum.de or protzer@helmholtz-muenchen.de (UP). Phone: 49.89.4140.6814; Email: karin.wisskirchen@tum.de (KW).

1. World Health Organization. *Global Hepatitis Report 2017*. Geneva, Switzerland: World Health Organization; 2017.
2. Trépo C, Chan HL, Lok A. Hepatitis B virus infection. *Lancet*. 2014;384(9959):2053–2063.
3. Lok AS, Zoulim F, Dusheiko G, Ghany MG. Hepatitis B cure: From discovery to regulatory approval. *J Hepatol*. 2017;67(4):847–861.
4. Thimme R, et al. CD8(+) T cells mediate viral clearance and disease pathogenesis during acute hepatitis B virus infection. *J Virol*. 2003;77(1):68–76.
5. Rehermann B, Nascimbeni M. Immunology of hepatitis B virus and hepatitis C virus infection. *Nat Rev Immunol*. 2005;5(3):215–229.
6. Belloni L, et al. IFN-α inhibits HBV transcription and replication in cell culture and in humanized mice by targeting the epigenetic regulation of the nuclear cccDNA minichromosome. *J Clin Invest*. 2012;122(2):529–537.
7. Liu F, et al. Alpha-interferon suppresses hepadnavirus transcription by altering epigenetic modification of cccDNA minichromosomes. *PLoS Pathog*. 2013;9(9):e1003613.
8. Tropberger P, Mercier A, Robinson M, Zhong W, Ganem DE, Holdorf M. Mapping of histone modifications in episomal HBV cccDNA uncovers an unusual chromatin organization amenable to epigenetic manipulation. *Proc Natl Acad Sci U S A*. 2015;112(42):E5715–E5724.
9. Guidotti LG, Rochford R, Chung J, Shapiro M, Purcell R, Chisari FV. Viral clearance without destruction of infected cells during acute HBV infection. *Science*. 1999;284(5415):825–829.
10. Lucifora J, et al. Specific and nonhepatotoxic degradation of nuclear hepatitis B virus cccDNA. *Science*. 2014;343(6176):1221–1228.
11. Allweiss L, et al. Proliferation of primary human hepatocytes and prevention of hepatitis B virus reinfection efficiently deplete nuclear cccDNA in vivo. *Gut*. 2018;67(3):542–552.
12. Bertoletti A, Ferrari C. Innate and adaptive immune responses in chronic hepatitis B virus infections: towards restoration of immune control of viral infection. *Gut*. 2012;61(12):1754–1764.
13. Bohne F, Protzer U. Adoptive T-cell therapy as a therapeutic option for chronic hepatitis B. *J Viral Hepat*. 2007;14 Suppl 1:45–50.
14. Ilan Y, Nagler A, Zeira E, Adler R, Slavin S, Shouval D. Maintenance of immune memory to the hepatitis B envelope protein following adoptive transfer of immunity in bone marrow transplant recipients. *Bone Marrow Transplant*. 2000;26(6):633–638.
15. Ilan Y, et al. Adoptive transfer of immunity to hepatitis B virus after T cell-depleted allogeneic bone marrow transplantation. *Hepatology*. 1993;18(2):246–252.
16. Lau GK, et al. Clearance of hepatitis B surface antigen after bone marrow transplantation: role of adoptive immunity transfer. *Hepatology*. 1997;25(6):1497–1501.
17. Qasim W, et al. Immunotherapy of HCC metastases with autologous T cell receptor redirected T cells, targeting HBsAg in a liver transplant patient. *J Hepatol*. 2015;62(2):486–491.
18. Bohne F, et al. T cells redirected against hepatitis B virus surface proteins eliminate infected hepatocytes. *Gastroenterology*. 2008;134(1):239–247.
19. Krebs K, et al. T cells expressing a chimeric antigen receptor that binds hepatitis B virus envelope proteins control virus replication in mice. *Gastroenterology*. 2013;145(2):456–465.
20. Gehring AJ, et al. Engineering virus-specific T cells that target HBV infected hepatocytes and hepatocellular carcinoma cell lines. *J Hepatol*. 2011;55(1):103–110.
21. Wisskirchen K, et al. Isolation and functional characterization of hepatitis B virus-specific T-cell receptors as new tools for experimental and clinical use. *PLoS ONE*. 2017;12(8):e0182936.
22. Kah J, et al. Lymphocytes transiently expressing virus-specific T cell receptors reduce hepatitis B virus infection. *J Clin Invest*. 2017;127(8):3177–3188.
23. Volz T, et al. The entry inhibitor Myrcludex-B efficiently blocks intrahepatic virus spreading in humanized mice previously infected with hepatitis B virus. *J Hepatol*. 2013;58(5):861–867.
24. Petersen J, et al. Prevention of hepatitis B virus infection in vivo by entry inhibitors derived from the large envelope protein. *Nat Biotechnol*. 2008;26(3):335–341.
25. Arzberger S, Hösel M, Protzer U. Apoptosis of hepatitis B virus-infected hepatocytes prevents release of infectious virus. *J Virol*. 2010;84(22):11994–12001.
26. Ko C, et al. Hepatitis B virus genome recycling and de novo secondary infection events maintain stable cccDNA levels. *J Hepatol*. 2018;69(6):1231–1241.
27. Wursthorn K, et al. Peginterferon alpha-2b plus adefovir induce strong cccDNA decline and HBsAg reduction in patients with chronic hepatitis B. *Hepatology*. 2006;44(3):675–684.
28. Gehring AJ, Protzer U. Targeting innate and adaptive immune responses to cure chronic HBV infection. *Gastroenterology*. 2019;156(2):325–337.
29. Xia Y, et al. Interferon-γ and Tumor necrosis factor-α produced by T cells reduce the HBV persistence form, cccDNA, without cytolysis. *Gastroenterology*. 2016;150(1):194–205.
30. Hoh A, et al. Hepatitis B virus-infected HepG2hNTCP cells serve as a novel immunological tool to analyze the antiviral efficacy of $CD8^+$ T cells in vitro. *J Virol*. 2015;89(14):7433–7438.
31. Sommermeyer D, et al. Chimeric antigen receptor-modified T cells derived from defined CD8 and $CD4^+$ subsets confer superior antitumor reac-

tivity in vivo. *Leukemia*. 2016;30(2):492–500.
32. Guidotti LG, Chisari FV. Noncytolytic control of viral infections by the innate and adaptive immune response. *Annu Rev Immunol*. 2001;19:65–91.
33. Xia Y, Protzer U. Control of hepatitis B virus by cytokines. *Viruses*. 2017;9(1):E18.
34. Koh S, Kah J, Tham CYL, Yang N, Ceccarello E, Chia A, et al. Nonlytic lymphocytes engineered to express virus-specific T-cell receptors limit HBV infection by activating APOBEC3. *Gastroenterology*. 2018;155(1):180–193.
35. Guidotti LG, et al. Cytotoxic T lymphocytes inhibit hepatitis B virus gene expression by a noncytolytic mechanism in transgenic mice. *Proc Natl Acad Sci U S A*. 1994;91(9):3764–3768.
36. Morgan RA, et al. Cancer regression and neurological toxicity following anti-MAGE-A3 TCR gene therapy. *J Immunother*. 2013;36(2):133–151.
37. Johnson LA, et al. Gene therapy with human and mouse T-cell receptors mediates cancer regression and targets normal tissues expressing cognate antigen. *Blood*. 2009;114(3):535–546.
38. Huang YH, et al. Core antigen expression is associated with hepatic necroinflammation in e antigen-negative chronic hepatitis B patients with low DNA loads. *Clin Vaccine Immunol*. 2010;17(6):1048–1053.
39. Ghani K, et al. Efficient human hematopoietic cell transduction using RD114- and GALV-pseudotyped retroviral vectors produced in suspension and serum-free media. *Hum Gene Ther*. 2009;20(9):966–974.
40. Zhang K, et al. Novel rtM204 Mutations in HBV Polymerase Confer Reduced Susceptibility to Adefovir and Tenofovir. *J Antivir Antiretrovir*. 2017;9(1):10–17.
41. Allweiss L, et al. Immune cell responses are not required to induce substantial hepatitis B virus antigen decline during pegylated interferon-alpha administration. *J Hepatol*. 2014;60(3):500–507.
42. Giersch K, et al. Hepatitis Delta co-infection in humanized mice leads to pronounced induction of innate immune responses in comparison to HBV mono-infection. *J Hepatol*. 2015;63(2):346–353.